A NEW MAP OF THE SOUTH POLE-AITKEN BASIN INCLUDING THE SOUTH POLE. C. M. Poehler[1], M. A. Ivanov[2], C. H. van der Bogert[1], H. Hiesinger[1], J. H. Pasckert[1], W. Iqbal[1], J. Wright[3], and J. W. Head[4], [1]Institut für Planetologie, Westfälische Wilhelms-Universität, Wilhelm-Klemm-Str. 10, 48149, Münster, Germany, c.poehler@uni-muenster.de, [2]Vernadsky Inst., RAS, Russia, [3]School of Physical Sciences, The Open University, Milton Keynes, MK7 6AA, UK, [4]Department of Earth, Environmental and Planetary Sciences, Brown University, Providence, RI 02912 USA.

Introduction: The South Pole-Aitken (SPA) basin is located on the lunar farside and is centered at ~53° S, 191° E. It is the largest [1-5] and oldest observable basin [6,7] on the Moon. Therefore, the timing of SPA formation gives valuable information on the formation and evolution of the lunar crust.

Here, we provide a comprehensive map (1:500K) of the SPA basin, including the South Pole region and parts of the Orientale basin, which is an extension of a map of the Apollo basin region [8]. The SPA basin and the South Pole are targets for future and ongoing robotic and human missions [e.g., 9–13], since the area potentially includes exposed mantle material [14, 15], sources of volatiles (e.g., pyroclastic deposits [6]), and permanently shadowed regions that may harbor ice or other volatiles [16]. For such missions, detailed studies of the geological history and setting of the region are necessary. Our map provides a comprehensive overview of the geology in the region (***Fig. 1***).

Methods: For large-scale mapping, we used the Lunar Reconnaissance Orbiter (LRO) Wide-Angle Camera (WAC) basemap (100 m/pixel). We used Narrow Angle Camera (NAC; 0.5 m/pixel) [17] and Kaguya (10 m/pixel) data for more detailed, smaller areas and for identifying specific features. We also used Clementine [18], M^3 [19], and Kaguya MI [20] data for spectral/compositional information. Topographic features were identified using Lunar Orbiter Laser Altimeter (LOLA) digital elevation products [21, 22] and a LOLA/Kaguya merged digital elevation model with a resolution of 59 m/pixel [23]. To mitigate the effect of low solar illumination angles at the pole, which cause significant shadows, we produced hillshade maps with various illumination conditions. We used PLANMAP mapping standards [24], an extension of USGS standards [25].

To begin with we used morphological appearance and albedo contrasts for identifying units and features. We determined relative ages for the units using morphological and stratigraphic evidence. In addition to relative dating of geologic units, we performed crater size-frequency distribution (CSFD) measurements and from these determined absolute model ages (AMAs) using the production and chronology functions of [26]. CSFD measurements were made using CraterTools [27] in ArcGIS, and we fitted the AMAs with Craterstats [28]. Detailed descriptions of the technique are given by [26, 29].

Geology: In our study area we defined three classes of geologic features: Basin materials, crater materials, and plains-forming materials.

Basin materials are related to the formation of the large basins in the area with the oldest and most dominant being the SPA basin. We also identified materials related to the Apollo, Schrödinger, and Orientale basins.

Crater materials are divided into different classes according to the state of degradation and shape of the craters. We dated several craters to obtain a framework for both the relative and absolute stratigraphy across the mapped area.

Plains-forming materials are characterized as relatively flat, smooth surfaces, and can be further divided into dark and light plains based on their albedoes.

SPA's rim is obscured by various later impacts and is degraded due to its old age. It appears most distinctively in the NW part of SPA, close to the Apollo basin. Here, we identify two topographic rings of SPA rim massifs. Around the South Pole, the morphological features become more difficult to interpret due to the low sun angle and extensive shadowing. We were able to find traces of the outer massif, but most of the inner massif seems to be destroyed by younger craters, if it existed in this area.

Acknowledgments: This paper is part of a project that has received funding from the European Union's Horizon 2020 research and innovation programme under grant agreement Nº776276 (PLANMAP).

References: [1] Stuart-Alexander (1978) USGS Map I-1047, 1978. [2] Spudis et al. (1994) *Science 266*, 1835-1839. [3] Hiesinger and Head (2004) *PLPSC 35*, 1164. [4] Shevchenko et al. (2007) *Solar Sys. Res. 41*, 447-462. [5] Garrick-Bethell and Zuber (2009) *Icarus 204*, 399-408. [6] Wilhelms (1987*) USGS SP-1348*, 302. [7] Hiesinger et al. (2012) LPSC 43, 2863. [8] Ivanov et al. (2018) *JGR Planets, 123*, 2585–2612. [9] Flahaut et al. (2019) *PSS.*, in press. [10] Steenstraet al. (2016) *Adv. Space Res. 58*, 1050–1065. [11] Allender et al. (2018) *Adv. Space Res. 63*, 692–727. [12] Hiesinger et al. (2019) *LPSC 50*, 1327. [13] Huang et al. (2018) *J. Geophys. Res., 123*, 1684 – 1700. [14] Melosh et al. (2017) *Geology, 45*, 1063-1066. [15] Yamamoto et al. (2010) Nature Geoscience 3, 533-536. [16] Nozette et al. (2001) *J. Geophys. Res., 106*, 23253– 23266. [17] Robinson et al. (2010) *Space Sci. Rev., 150*, 81–124. [18] Pieters et al. (1994). *Science, 266*, 1844–1848. [19] Isaacsom et al. (2013). *JGR, 118*, 369–381. [20] Ohtake et al (2013*) Icarus, 226*, 364–374. [21] Smith et al. (2010) Icarus, 283, 70-91. [22] Smith et al. (2010) *Geophys. Res. Lett.*, 37, L18204. [23] Scholten et al. (2012) *JGR, 117*, E00H17. [24] wiki.planmap.eu/display/public/D2.1-public. [25] FGDC (2006). FGDC-STD-013-2016. [26] Neukum et al. (2001) *Space Sci. Rev. 96*, 55–86. [27] Kneissl et al. (2011) *PSS, 59*, 1243–1254. [28] Michael and Neukum (2010) *EPSL, 294*, 223–229. [29] Hiesinger et al. (2000) *JGR, 105*, 29239–29276.

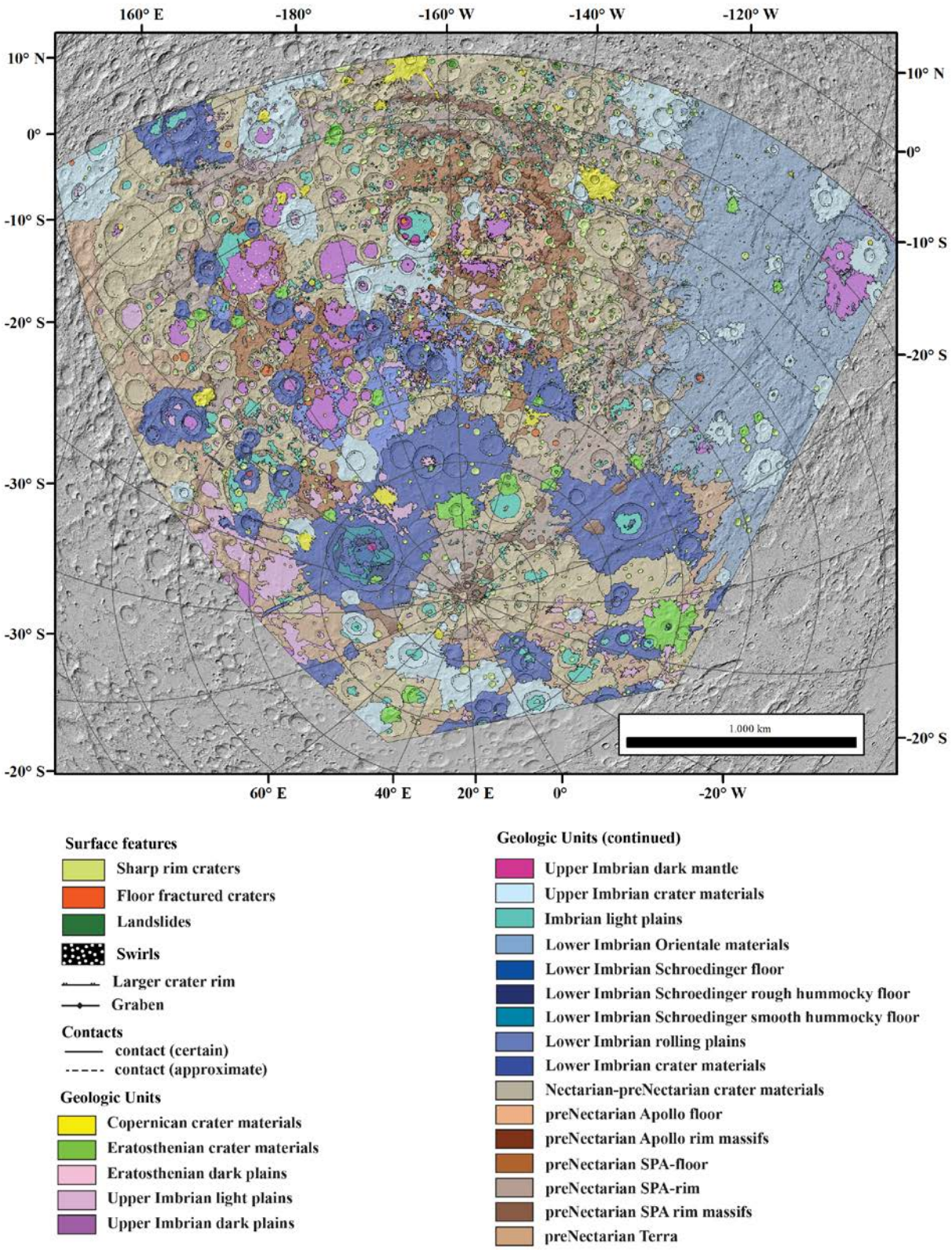

Figure 1. *Preliminary geological map of the lunar South Pole and the South Pole-Aitken basin at a scale of 1:500,000 in Lambert projection centered at 157.5° S and 53° E. The background image is a hillshade map compiled from a LOLA global DEM.*